Performance Characteristics of Hydrogen Peroxide/Kerosene Staged-Bipropellant Engine with Axial Fuel Injector

Sungkwon Jo*
Korea Advanced Institute of Science and Technology, Daejeon 305-701, Republic of Korea
Sungyong An[†]
Korea Institute of Nuclear Safety, Daejeon 305-338, Republic of Korea
Jonghak Kim[‡] and Hosung Yoon[§]
Space Solutions Company, Ltd., Daejeon 305-509, Republic of Korea
and
Sejin Kwon[¶]
Korea Advanced Institute of Science and Technology, Daejeon 305-701, Republic of Korea

A 1200 N vacuum-thrust-class staged-bipropellant engine that uses decomposed hydrogen peroxide as an oxidizer and kerosene as a fuel was developed and tested with the aim of investigating an axial fuel injector integrated with a distributor. This fuel injector geometry, where fuel is injected into the turbulent flow of decomposed hydrogen peroxide, was tested to evaluate the influence of the designed injector on engine performance with respect to the equivalence ratio, the pattern of fuel injection orifices, and the characteristic length L^*. For characteristics such as autoignition and stable combustion, firing tests over a wide range of equivalence ratios from 0.26 to 1.86 were carried out. Autoignition was successfully achieved under all experimental conditions. The pressure rising time from monopropellant to bipropellant mode and the pressure fluctuation in the combustion chamber were approximately 100 ms and less than ±1.1%, respectively. In the parametric study, the characteristic velocity c^* and its efficiency were influenced by the pattern of fuel injection, whereas varying the orifice diameter had no effect. The effect of L^* was also estimated, and the c^* efficiency was measured to be over 95% for all equivalence ratios at an L^* of 1.20 m.

Nomenclature

C_{d_f} = discharge coefficient for fuel
C_{d_o} = discharge coefficient for oxidizer
c^* = characteristic velocity, m/s
L^* = characteristic length, m
ϕ = equivalence ratio

I. Introduction

THE current representative standard for high-performing storable bipropellants is the combination of nitrogen tetroxide and monomethylhydrazine, even though both chemicals pose significant health hazards. With growing concerns about the environment and health hazards, low-toxicity storable liquid propellants have attracted considerable interest for enhancing safety and reducing costs of aerospace propulsion systems [1]. As part of these efforts, the combination of hydrogen peroxide and a liquid hydrocarbon-based fuel has again come under focus since the mid-1990s, even though this combination is one of the oldest in modern rocket history [2–5].

*Graduate Student, Division of Aerospace, 373-1, Guseong-dong, Yuseong-gu; earthcsk@kaist.ac.kr. Member AIAA.
†Senior Researcher, 34, Gwahak-ro, Yuseong-gu; k975asy@kins.re.kr.
‡Researcher, 1321, Gwanpyeong-dong, Yuseong-gu; whdgkr00@hanmail.net.
§Researcher, 1321, Gwanpyeong-dong, Yuseong-gu; hoffman48@naver.com.
¶Professor, Division of Aerospace, 373-1, Guseong-dong, Yuseong-gu; trumpet@kaist.ac.kr. Member AIAA.

When hydrogen peroxide is used as an oxidizer, there are generally two methods for fuel combustion [6]. The first method is referred to as staged-bipropellant combustion and uses decomposed hydrogen peroxide, which is obtained from a catalytic reaction that gives oxygen and water vapor, releasing high thermal energy. For 90%-concentrated hydrogen peroxide by weight, the adiabatic decomposition temperature of the product gases is approximately 749°C. Hence, by injecting liquid fuel into a hot gas stream, autoignition can be achieved [7–9]. The other method uses liquid hydrogen peroxide and liquid fuel along with a catalyst that becomes hypergolic in the presence of hydrogen peroxide [10–12]. All of the previous rockets that have flown in the past, such as the Gamma-series and LR-40 engines, used decomposed product gases of hydrogen peroxide [13,14]. This approach has a number of advantages. Simple bipropellant systems can be designed by dividing fuel and oxidizer injectors. In addition to avoiding a complex injector head, the product gases rapidly atomize and vaporize a fuel fed in the combustion chamber due to the high temperature and momentum of the decomposed hydrogen peroxide.

Prior efforts mostly focused on autoignition of hydrocarbon-based fuels in decomposed hydrogen peroxide with various fuel injector geometries. Walder and Purchase investigated the effect on the autoignition temperature for a number of complex injector designs using swirl jet, straight orifice, and combined swirl and straight injection [15]. Coxhill et al. developed a small bipropellant thruster that uses a spray-jet injector for a fuel [7]. Sisco et al. used a transverse fuel injector to investigate the effects of hydrogen peroxide concentration, contraction ratio, and equivalence ratio on autoignition of JP-8 fuel [8]. Although there were several valuable results, more efforts toward understanding the system, especially the injector, are needed, because the injector in a bipropellant propulsion system controls the performance and combustion instabilities.

Upon decomposition of hydrogen peroxide in the presence of a catalyst, a pressure drop occurs along the catalyst bed in the catalyst reactor of a staged-bipropellant engine. To prevent the catalyst bed from breaking, the catalyst should be blocked by a distributor at the end of the reaction chamber. A distributor is usually a metal plate

with numerous holes. These holes are covered with a metal mesh with gaps smaller than the diameter of the catalyst support granules. Decomposed hydrogen peroxide passes through these holes of the distributor leading to complex flow at the end of the reaction chamber. To use this turbulent flow of decomposed hydrogen peroxide, the axial fuel injector was designed to be integrated with the distributor. This study is focused on investigating the influence of injecting a fuel with an axial injector in the complex flow region of decomposed hydrogen peroxide.

This paper presents experiment results showing the effects of the equivalence ratio, the pattern of fuel injection orifices, and the variation of characteristic length on the performance of a staged-bipropellant combustor. Because a fuel is axially injected into the complex flow of decomposed hydrogen peroxide, the autoignition feasibility and instability in the combustor were investigated over a wide range of equivalence ratios. Three L^* conditions were considered in this study to provide an appropriate L^* value for high performance of the designed staged-bipropellant engine.

II. H_2O_2/Kerosene Staged-Bipropellant Engine

A 1200 N vacuum-thrust-class staged-bipropellant engine with a nominal chamber pressure of 30 bar was designed and fabricated. Its main components are the catalyst, catalyst reactor, oxidizer and fuel injectors, and combustor. Each part was designed to be modular for easy replacement with other geometries. The schematic drawing of the designed staged-bipropellant engine is shown in Fig. 1.

A. Catalyst and Catalytic Reactor

To achieve complete decomposition of all the hydrogen peroxide fed, selecting the appropriate catalyst and size of the catalytic reactor is very important. The selected catalyst should not only completely decompose all of the hydrogen peroxide fed but also sustain high temperatures of approximately 749°C for 90 wt% hydrogen peroxide. A noble metal such as platinum or silver generally shows better performance in reaction with hydrogen peroxide than other catalysts. However, manganese catalysts are also broadly used due to their cost effectiveness.

In this study, MnO_2 was used as a catalyst due to its superior reactivity [16]. Pb was selected as an additive material to enhance the reactivity of MnO_2 [17]. Bimodal-type Al_2O_3 was used as the catalytic support; it has a surface area to mass ratio of approximately 255 m^2/g. Because the catalytic support size can affect the activity of a catalyst, according to An et al. [18], granules with mesh sizes of 10–16 (1.18–2.0 mm) were prepared from the Al_2O_3 pellets. Both $NaMnO_4$ and $Pb(NO_3)_2$ were used as precursors for MnO_2 and PbO, respectively; they were mixed so that the molar weights of Mn and Pb were identical. The catalyst obtained from the mixed precursors was deposited on Al_2O_3 granules by the wetness impregnation method. Impregnation was followed by drying (90°C for 12 h), calcination (500°C for 4 h), and drying (90°C for 12 h) again. After calcination, the catalyst was washed with water to remove Na^+ ions and impurities.

The catalyst bed should be of an optimum length to obtain the desired adiabatic temperature at the end of the catalytic reactor.
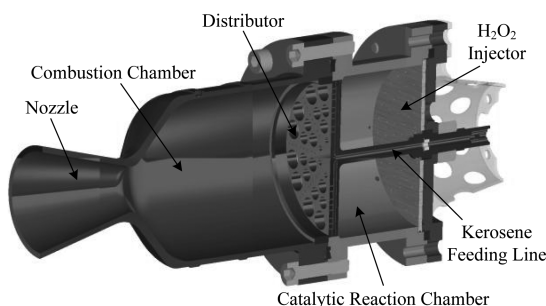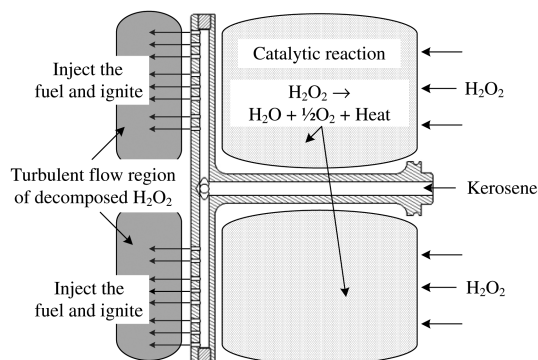

Fig. 2 Concept of fuel injection into turbulent flow region of decomposed hydrogen peroxide.

According to An and Kwon [19], the length of the reaction chamber can be estimated from the decomposition capacity of the catalyst bed, which is defined as the propellant mass flow rate divided by the catalyst bed volume. The decomposition capacity depends on the catalyst material, catalytic support size, concentration of hydrogen peroxide, etc. In this study, the decomposition capacity of MnO_2 with added Pb was assumed to be approximately 3.75 $g/cm^3 \cdot s$, which was confirmed experimentally. The catalytic reactor was designed to completely decompose hydrogen peroxide and have a mass flow rate of approximately 366.4 g/s. The dimensions of the reactor were a 60 mm diameter and 35 mm length, and there is a pressure drop through the reaction chamber.

B. Axial Fuel Injector

The primary purpose of this study was to design and to investigate an axial fuel injector integrated with a distributor that can inject the fuel into the turbulent flow of decomposed hydrogen peroxide. It was motivated because a distributor is necessary to fix a catalyst bed in a staged-bipropellant combustor, and autoignition can be enhanced by flame-holding geometries to maximize turbulent mixing time between a fuel and an oxidizer. Because the turbulent flow of decomposed hydrogen peroxide occurs downstream of the distributor, enhanced mixing and autoignition can be obtained by injecting the fuel into the turbulent flow region. The basic concept of the designed fuel injector integrated with a distributor is shown in Fig. 2. Axial fuel injection was adopted due to its simplicity and convenience for changing the location of the fuel orifices. The kerosene passes through the stainless steel pipe located at the center of the catalytic reactor, spreads out radially inside of the distributor, and is finally injected into the combustion chamber through the fuel orifices.

The orifices of the fuel and oxidizer were designed identically at 45° intervals on the injector face, as shown in Fig. 3. The orifices for the decomposed hydrogen peroxide were designed considering fabrication limitations, and the diameters are 2.0–7.0 mm. For the fuel orifices, there are eight branch lines inside the distributor to distribute the fuel in the radial direction. To investigate the effects of
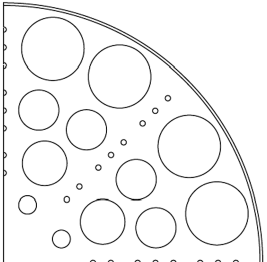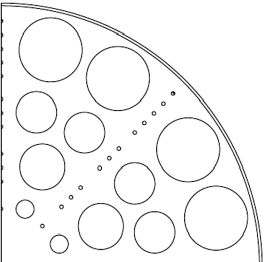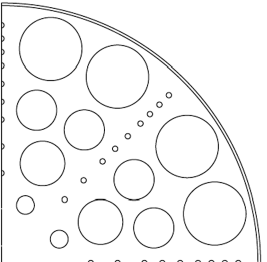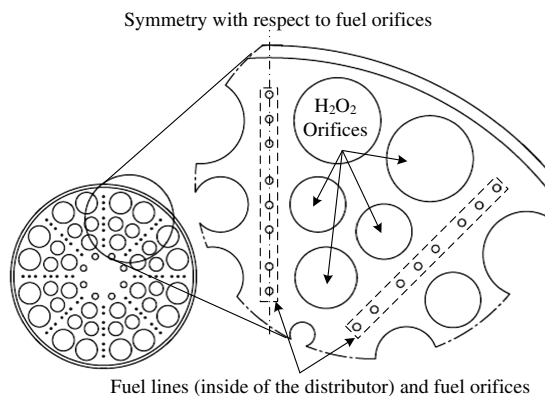

Fig. 1 Schematic of designed H_2O_2/kerosene staged-bipropellant engine.

Fig. 3 Schematic of fuel injector face and detailed view.

Table 1 Fuel injection pattern and properties

Parameter	Case 1	Case 2	Case 3
Pattern			
Orifice number	8 per 45°	12 per 45°	9 per 45°
Orifice diameter, μm	600	400	600
Average values at each fuel orifice (relative percentage compared with case 1)			
Injection velocity [a]	35.7 m/s (100%)	53.6 m/s (150%)	31.7 m/s (88.9%)
Mass flow rate [a]	0.813 g/s (100%)	0.542 g/s (66.7%)	0.722 g/s (88.9%)

[a]Note that the injection velocity and mass flow rate at each fuel orifice were simply determined by using the designed fuel mass flow rate and orifice area.

the fuel injection pattern, the patterns are classified by the location and diameter of the fuel orifices, as shown in Table 1. Case 1 has almost even gaps between the fuel orifices along the radial direction. Compared with case 1, cases 2 and 3 examined the size and location effects, respectively, of fuel orifices. In particular, case 3 was intended to concentrate the fuel orifices around the outer side of the fuel branch line, because a large amount of the oxidizer passes through the outside of the distributor due to the relative difference in orifice size.

C. Combustor

The combustor is composed of a combustion chamber and a conical nozzle. The combustion chamber has a wall thickness of 2.0 mm and a safety factor of 1.5 using the properties of stainless steel 304. The combustion chamber volume was determined by the value of the characteristic length L^* of 0.95 m. Two blocks can extend the combustion chamber length by being inserted between the combustion chamber and catalytic reactor; they change the L^* to 1.07 and 1.20 m. The characteristic length L^* is defined as the ratio of the combustion chamber volume from the fuel injector face to the plane of the nozzle throat to the nozzle throat cross-sectional area. In other words, the catalyst bed is excluded from the calculation of L^* in this study. Dimensions of the 15° conical nozzle were designed based on one-dimensional equilibrium calculations using NASA's Chemical Equilibrium and Applications program [20]. Table 2 shows a

summary of the designed engine, including the catalyst bed, axial fuel injector, combustion chamber, and nozzle.
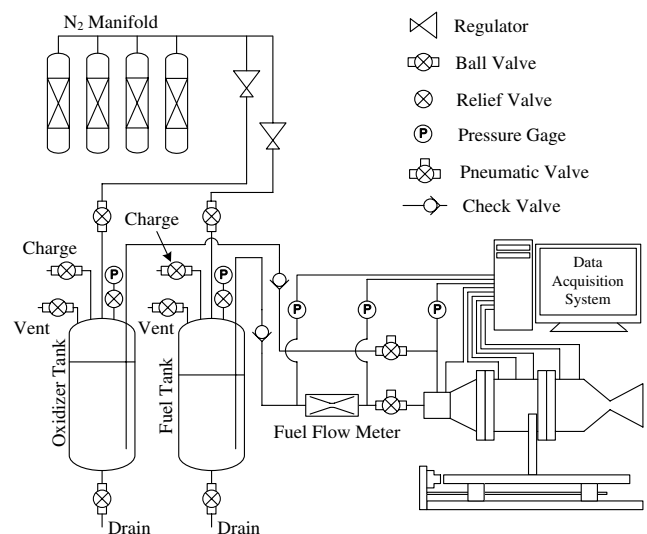
III. Experimental Setup

Hydrogen peroxide with a concentration of 90 wt% was used in all of the experiments. The quality of hydrogen peroxide was nearly in accordance with the requirements of MIL-PRF-16005F [21], which defines the maximum allowable impurities for rocket-grade hydrogen peroxide. The densities were 1380 kg/m³ for hydrogen peroxide and 804 kg/m³ for kerosene at 25°C.

Hydrogen peroxide and kerosene were pressurized with a regulated nitrogen gas manifold system. The propellants and purging nitrogen gas were controlled by a pneumatic actuator operated using a solenoid valve. Each pneumatic actuator was linked to a timer in order for precise operation at the designated time. A data acquisition card and signal conditioning extension for instrumentation modules (10 kHz filter) from National Instruments were used to measure the temperature and pressure. The sampling rate for data acquisition was 1000 samples/s. K-type thermocouples with an open junction were used to measure the temperature of the product gases in the catalyst bed. Five pressure transducers of three different types [35 bar max ±0.12% accuracy, 50 bar max ±0.04% accuracy, and 70 bar max ±0.15% accuracy] were used to measure pressures in the combustion chamber, the manifold of hydrogen peroxide, the injector face of hydrogen peroxide, and the upstream and downstream of an orifice-type flow meter for the fuel. The schematic of the

Table 2 Baseline of designed engine

Parameter	Value	Unit
General		
Chamber pressure	30	bar
Vacuum thrust	1200	N
Characteristic velocity	1597.8	m/s
Characteristic length	0.95	m
Total mass flow rate	0.417	kg/s
Mixture ratio	7.2	
Catalyst reactor		
Reactor diameter	60	mm
Reactor length	35	mm
Catalyst capacity	3.75	g/cm³ · s
Catalyst bed loading	13.12	g/cm² · s
Combustion chamber		
Chamber diameter	60	mm
Chamber length	66.25	mm
Nozzle		
Throat diameter	16.83	mm
Contraction ratio	12.75	
Exit diameter	37.44	mm
Expansion ratio	4.95	

Fig. 4 Schematic of experimental setup.

experimental setup for investigating the H_2O_2/kerosene staged-bipropellant engine is shown in Fig. 4.

Once the designed engine was fabricated, water-flow tests were performed to confirm whether the orifices for each propellant were unclogged and the injection direction was axial at each orifice. During this test, the discharge coefficient C_{d_o} and its error for the hydrogen peroxide injector were obtained from dozens of water-flow tests. For the fuel, an orifice-type mass flow meter was installed separately, because measuring the pressure in the fuel manifold is difficult due to complex geometry. Using an identical procedure for hydrogen peroxide, the discharge coefficient C_{d_f} and its error for the fuel were also obtained; the mass flow rate of each propellant can be calculated by measuring the pressure difference between the up-stream and downstream of the injector for hydrogen peroxide and of the measurement orifice for kerosene using Eq. (1):

$$\dot{m} = nC_d A \sqrt{2\rho\Delta P} \qquad (1)$$

where $\dot{m}$ is the mass flow rate, n is the number of orifices, A is the area of an orifice, ρ is the propellant density, and ΔP is the pressure difference across an injector or measurement orifice.

IV. Testing Results

Before the firing tests, the catalyst bed was first tested in monopropellant mode by injecting only hydrogen peroxide. The tests were carried out by increasing the mass flow rate of hydrogen peroxide; a rate of approximately 412.9 g/s was successfully decomposed at a temperature of approximately 728°C at the end of catalyst bed. Considering that the adiabatic temperature of 90 wt% hydrogen peroxide is 749°C, the decomposition efficiency and catalyst capacity were calculated as 97.2% and 4.2 g/cm³ · s, respectively. Because this is sufficient to decompose the designed mass flow rate, which was 366.4 g/s hydrogen peroxide, a full decomposition condition was assumed in the firing tests. During the firing tests, the fuel was injected after an initial 1.0 s for introducing hydrogen peroxide to make the temperature condition at the end of catalyst bed as identical as possible.

The first firing test was performed under the condition of 80% total mass flow rate in fuel-lean condition to reduce the combustion chamber pressure of the combustion chamber. These tests are to ensure safety and check the experimental procedure and engine, as well as investigate the autoignition under extremely fuel-lean conditions. The procedure takes a total of 2 s, i.e., an initial 1 s for only hydrogen peroxide injection and the following 1 s for firing. However, a flame was observed after the end of the procedure due to additional injection of the fuel in the manifold, resulting from residual pressure by the relatively slow pressure release time of hydrogen peroxide. The remaining fuel in the combustion chamber may lead to unexpected ignition or damage to the bipropellant engine. Thus, the experimental sequence was safely modified so that once the fuel valve is closed, it is followed by 1 s of nitrogen gas and hydrogen peroxide to purge the fuel in the manifold and take the remaining fuel away from the combustion chamber, respectively.

After modifying the experiment procedure, all of the firing tests were successfully completed without damage to the engine. Over 42
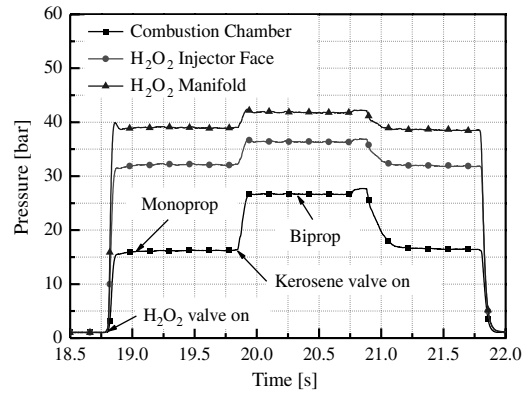

Fig. 6 Pressure variations of combustion chamber, H_2O_2 injector face, and manifold (test conditions: fuel injection pattern = case 3, $\phi = 1.03$, and $L^* = 1.07$ m).

firing tests were conducted to investigate the instability of the ignition and performance with respect to the equivalence ratio, axial fuel injection pattern, and characteristic length. One of the firing tests is shown in Fig. 5. First, fuel injectors with different orifice patterns were tested under fuel-rich conditions with a characteristic length of 0.95 m. Based on the pattern variation results, the fuel injector showing the highest performance was employed to estimate the effect of the characteristic length. After each test, inspection of the engine, including the nozzle throat, chamber diameter, and fuel injector, provided no signs of erosion or damage.

The pressure profiles in the combustion chamber, injector face, and feeding manifold for hydrogen peroxide are shown in Fig. 6. During the first 1 s period of hydrogen peroxide injection only, the monopropellant pressure was established as 16.2 bar in the combustion chamber. The fuel was supplied for the next 1 s period, resulting in a chamber pressure increase to 26.7 bar. The chamber pressure in bipropellant mode differed due to the equivalence ratio and combustion efficiency but typically increased approximately 60% from monopropellant to bipropellant modes. There was a pressure peak at the end of the bipropellant mode due to a purging sequence by nitrogen gas with higher pressure than that of the fuel supply. After the following monopropellant mode for the 1 s period to remove the remaining fuel in the combustion chamber, all pneumatic valves were closed. The results under all experimental conditions showed similar trends in pressure variation.

Chamber pressures with different equivalence ratios are overlaid, as shown in Fig. 7. Each pressure variation showed almost the same rate, which indicates that autoignition occurred smoothly. Because the primary goal of this study was focused on investigating the axial fuel injector integrated with a distributor, the delay time in mono-propellant mode (which is mainly related to the catalyst, catalyst support, catalyst bed design, etc. [18]) was not considered. The delay time from monopropellant to 90% bipropellant steady-state level in
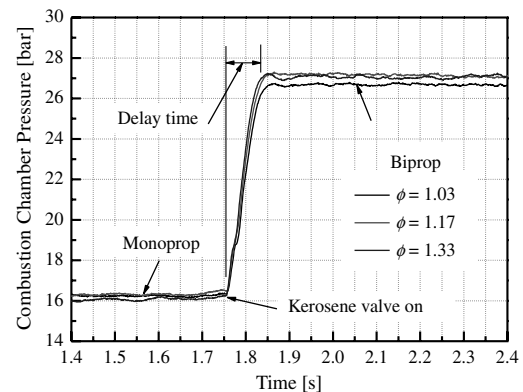

Fig. 5   Test fire of designed engine.

Fig. 7 Pressure variation of combustion chamber (test conditions: fuel injection pattern = case 3, and $L^* = 1.07$ m).

the pressure profile was approximately 80 ms, which is substantially greater than the less-than-50-ms delay for JP-8/hydrogen peroxide using a transverse fuel injector in a dump combustor [8]. In the staged-bipropellant system, the delay time generally corresponds to the time required to fill the fuel manifold as the designed pressure drop across the fuel injector and to vaporize the fed fuel. In addition, the delay increase in this study is most likely the result of turbulent flow around the distributor, whereas the other study used a straight flow of decomposed hydrogen peroxide.

The pressure fluctuation, which can be calculated by the difference between maximum and minimum pressure values dividing the steady-state pressure in the combustion chamber, was recorded as less than $\pm 1.1\%$ of the steady-state pressure; this indicates that combustion was quite stable compared with other studies that used decomposed hydrogen peroxide: less than $\pm 5.0\%$ with a spray-jet fuel injector [7] and about $\pm 8.5\%$ calculated from the pressure graph with a transverse fuel injector [8]. When hypergolic fuels with hydrogen peroxide using a liquid–liquid injector are considered, the pressure fluctuations were reported to be ± 4.0 to $\pm 10.0\%$ [10–12]. The axial fuel injector designed to inject the fuel into a turbulent flow of decomposed hydrogen peroxide clearly shows considerable stability during the combustion process, at least within the test sampling frequency of 1000 Hz. The stable combustion pressure may be due to the number of fuel orifices distributed all over the injector surface, because the only distinguishing difference with prior studies was the fuel injection type.

To provide a degree of accuracy in the measured and calculated results, the uncertainty analysis outlined by Coleman and Steele [22] was performed with the assumption that the primary error in performance was related to the mass flow rate of each propellant, pressure transducers, and tolerance of the nozzle throat. The errors of the mass flow rates for each propellant were calculated with the discharge coefficient error and were shown to be less than $\pm 3.1\%$ for hydrogen peroxide and less than $\pm 3.6\%$ for kerosene. Based on the information supplied by the instrumentation manufacturers and nozzle throat tolerance, the error of the measured pressure and dimension at the throat were as assigned values of approximately 0.1% and ± 0.01 mm, respectively. All of the tested points were calculated by the uncertainty analysis and assumptions, which are indicated as error bars on the following graphs.

A. Autoignition Test Under Fuel-Lean Conditions

Firing tests under fuel-lean conditions were performed to check the overall systems and investigate the autoignition feasibility of kerosene in the designed fuel injector system. Autoignition under extremely fuel-lean conditions was successfully achieved, and c^* increases with increasing equivalence ratio, as shown in Fig. 8. Based on the calculation of theoretical c^* using the combustion chamber pressure and equivalence ratio taken from the experimental results, the c^* efficiencies were at or over 100% under the condition of reduced total mass flow rate, which was approximately 332.6 g/s

(about 80% of the designed total mass flow rate) with a standard deviation of $\pm 2.2\%$. The error under the equivalence ratio of below 0.5 was quite large due to the mass flow rate. This is due to measurement error for the fuel, because the orifice diameter for measuring the fuel mass flow rate is too large to be sensitive to extremely low flow rates of below about 20 g/s. Although the absolute performance in this test is not acceptable due to the reduced total mass flow rate and error, autoignition under extremely fuel-lean conditions as low as 0.26 was confirmed to be achievable using the axial fuel injector integrated with a distributor.

B. Fuel Injector Pattern Variations

The diameter and pattern of the fuel orifices influence the engine performance, because they control the global and local equivalence ratios and the time to vaporize fuel with decomposed hydrogen peroxide. Three different fuel injectors were tested for an average total mass flow rate of approximately 410.5 g/s with an average

a) Pattern case 1

b) Pattern case 2

c) Pattern case 3

Fig. 9 Characteristic velocity and its efficiency with respect to fuel orifice patterns ($L^* = 0.95$ m).

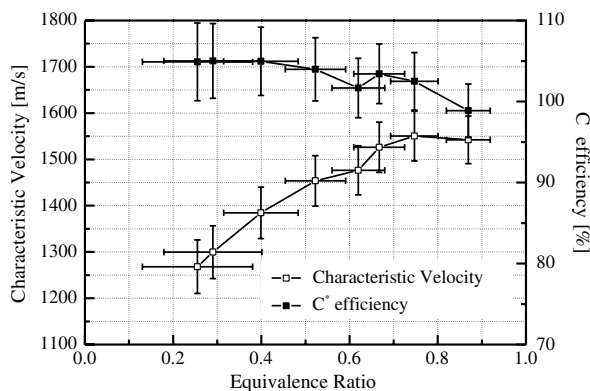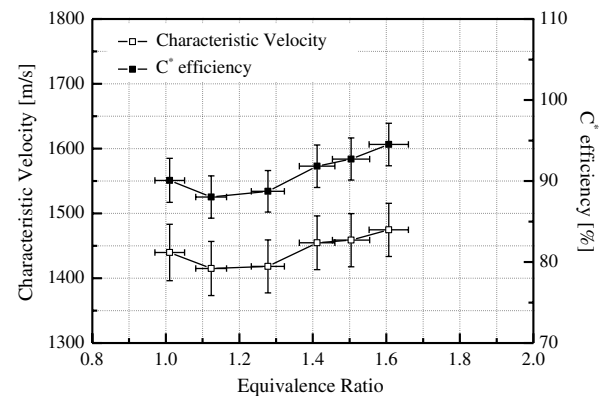Fig. 8 Characteristic velocity and its efficiency under fuel-lean conditions (test conditions: fuel injection pattern = case 1, and $L^* = 0.95$ m).
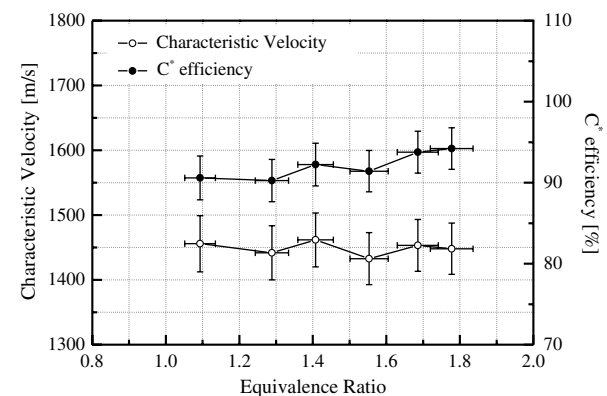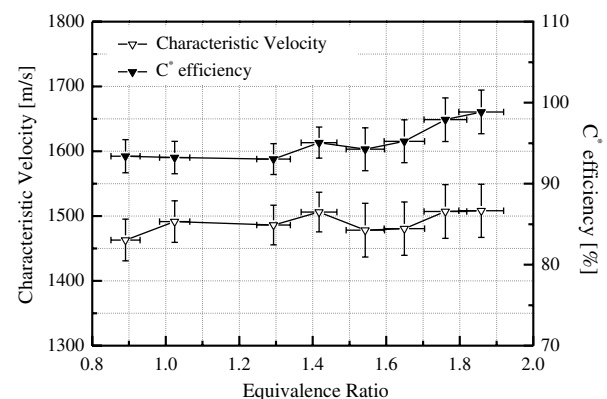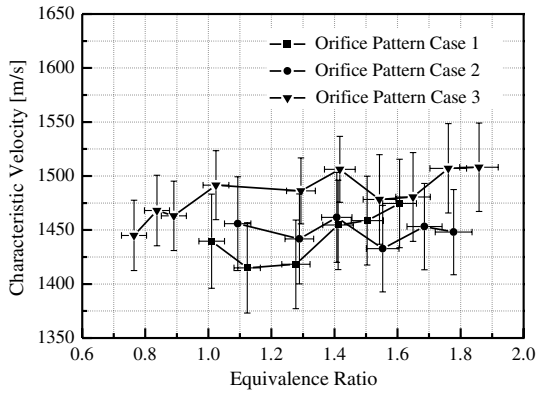
Fig. 10 Comparison of characteristic velocity with respect to fuel injection patterns.

standard deviation of $\pm 1.9\%$ under all conditions. As shown in Fig. 9 for each pattern, the results for c^* and the efficiency showed maximum errors of ± 43.4 m/s and $\pm 2.7\%$, respectively. Although the highest value of c^* theoretically occurred near the equivalence ratio of 1.1, the c^* results either did not change or increased with increasing equivalence ratio. Ideal combustion is believed to not be achievable in the chamber because the local mixing ratio may not match the global mixing ratio taken from the mass flow rates of the propellants.

Figure 10 compares c^* for different injector geometries, and theoretical c^* corresponding with the test conditions was shown in Fig. 11 for comparison. First, the effect of the time to atomize and vaporize a fuel by changing the orifice diameter was investigated by comparing the case 1 and case 2 patterns. The average mass flow rates at each fuel orifice were 0.813 and 0.542 g/s at diameters of 0.6 and 0.4 mm, respectively. The average c^* efficiency for a 0.4 diameter increased by about 1.0%. However, considering the average error of about $\pm 2.5\%$, it was concluded that there is no noticeable performance change, and an axial injector with an orifice diameter of 0.6 mm and mass flow rate of about 0.8 g/s per each orifice can sufficiently atomize and vaporize an injected fuel with decomposed hydrogen peroxide.

When comparing the injector patterns for cases 1 and 3, the combustion performance increased by approximately 4.1% for the average c^* efficiency by changing the locations of the fuel orifices. The fuel orifices for the case 3 pattern were intentionally located so that the local mixing ratios along the radial direction were close to the designed oxidizer-to-fuel ratio according to the area ratios between the oxidizer and fuel orifices. The effect of having an additional orifice on the radial line may naturally affect the performance due to the relatively low injection velocity and reduced fuel mass per orifice. However, since case 2 showed no noticeable change in performance compared with case 1, the location change of fuel orifices may be a primary reason for the enhanced combustion performance. Therefore, the performance of the axial fuel injector integrated with a
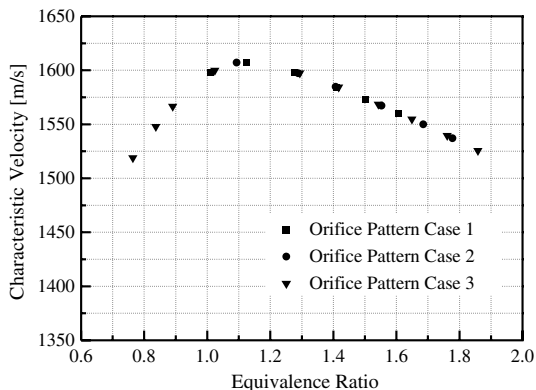
distributor may be affected by global as well as local mixing ratios in the combustion chamber and improved by considering the turbulent flow aspect of decomposed hydrogen peroxide and the location of fuel orifices.
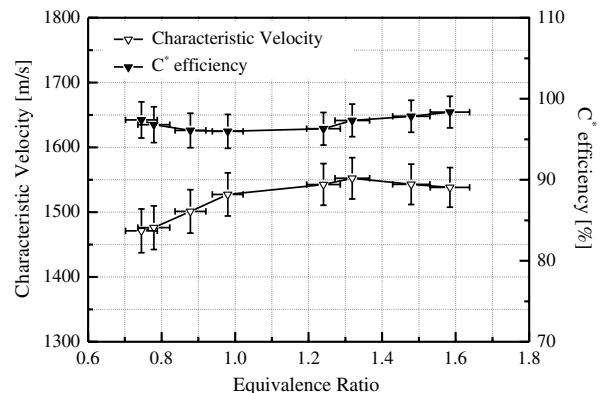
C. Characteristic Length Variations

The characteristic length L^*, which affects the design of the combustion chamber volume, is one of the representative factors that determine engine performance. With increasing L^*, the combustion chamber residence time increases, which leads to enhanced atomization, vaporization, mixing, and ignition of propellants. However, L^* should be optimized, because a high L^* results in a heavier engine and greater chamber wall surface that needs to be cooled. To provide the appropriate L^* value, the c^* and its efficiency were tested with the case 3 fuel injector at L^* of 0.95, 1.07, and 1.20 m, as shown in Figs. 9c and 12. Although the error of the c^* efficiencies was approximately $\pm 2.1\%$, which may have disturbed the measured trend of L^* variation, the average c^* efficiency increased by about 1.0% with increasing L^*. c^* also increased, but the variation from 1.07 to 1.20 m of L^* was not noticeable, as shown in Fig. 13. At the designed equivalence ratio of approximately 1.1, which showed the highest theoretical performance, the c^* efficiency was about 93.1, 96.6, and 96.2% at L^* of 0.95, 1.07, and 1.20 m, respectively. The results show that a combustion chamber with L^* of above 1.07 can ensure a c^* efficiency of over 95%.

A study employed four spray-jet fuel injectors with L^* of approximately 1.91 m; the average c^* efficiency was reported as 90.9%, but autoignition when L^* was 1.22 m did not occur because the design of the combustor had no flame holder [7]. Combustor geometry without a flame holder is believed to need a much greater volume to allow atomization and vaporization of a fuel. A study that used a typical transverse fuel injector in a staged combustor with a flame holder reported a c^* efficiency of about 94% at L^* of 1.02 m [8]. Compared with the results of other studies that used decomposed
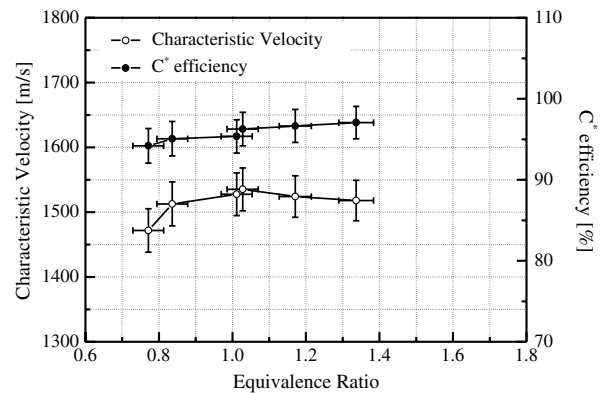
a) $L^* = 1.07$ m

b) $L^* = 1.20$ m

Fig. 12 Characteristic velocity and its efficiency with respect to characteristic lengths (case 3 pattern).

Fig. 11 Comparison of theoretical characteristic velocity with respect to fuel injection patterns.
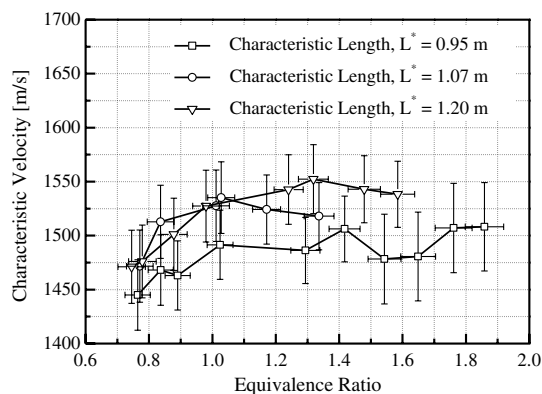
Fig. 13 Comparison of characteristic velocity with respect to characteristic lengths.

hydrogen peroxide, the axial fuel injector designed in this study can function as a flame holder, and an L^* of 1.0 m can be selected to achieve a c^* efficiency of over 90% in the design of a staged-bipropellant engine, regardless of whether the injector in this study or a transverse injector is used.

V.   Conclusions

A 1200-N-class vacuum-thrust H_2O_2/kerosene staged-bipropellant engine was designed to investigate the feasibility and performance of an axial fuel injector integrated with a distributor that can inject the fuel into the turbulent flow of decomposed hydrogen peroxide. Smooth, repeatable autoignition was successfully demonstrated with the designed axial fuel injector over a wide range of equivalence ratios from 0.26 to 1.86. Typical rise times from monopropellant to bipropellant mode were less than 100 ms, indicating that the response time was somewhat slow. This is likely due to the additional time induced by the turbulent flow near the distributor and extended fuel manifold volume to distribute the fuel inside the distributor. On the other hand, the pressure fluctuation in the combustion chamber was less than $\pm1.1\%$ under both monopropellant and bipropellant modes, which means that the combustion process was quite stable.

Fuel injection pattern variations were tested to identify the influences on the engine performance. Patterns classified by the location and diameter of the fuel orifices were fabricated and tested. Although a noticeable change could not be found when testing different diameters of the fuel orifices, varying the fuel injection patterns resulted in an increase in c^* efficiency over a wide range of equivalence ratios. Since the fuel jet trajectory affected by the streamline of decomposed hydrogen peroxide is changed by the locations of the fuel injection, the global and local equivalence ratios may be close to the stoichiometric condition when the locations of the fuel injection orifices are rearranged to the outer region of the fuel injector face.

Using the case 3 fuel injection pattern, which showed the highest c^* efficiency in prior tests, the test for L^* variations endeavored to determine the optimized value for high c^* efficiency. With increasing L^*, c^* efficiency enhanced in accordance with theoretical expectations, but there was no obvious improvement at an L^* higher than 1.07 m (e.g., 1.20 m). The c^* efficiency was approximately 96.6% at the conditions of the equivalence ratio of 1.1 selected in this study and L^* of 1.07 m. Considering the measured error, over 90% c^* efficiency was concluded to be achievable by applying an L^* of above 1.07 m in the design of a staged-bipropellant engine using an axial fuel injector integrated with a distributor.

Acknowledgment

References

[1] Murphy, T. H., Coffman, P. E., Jensen, J. J., and Hoffman, C. S., "Storable Liquid Propellant Usage: Trends in Non-Toxic Propulsion," *49th International Astronautical Congress*, Melbourne, Australia, International Astronautical Federation, Paris, Oct. 1998.

[2] Ventura, M., and Garboden, G., "A Brief History of Concentrated Hydrogen Peroxide Uses," 35th AIAA/ASME/SAE/ASEE Joint Propulsion Conference and Exhibit, Aliso Viejo, CA, AIAA Paper 1999-2739, June 1999.

[3] Ventura, M., and Mullens, P., "The Use of Hydrogen Peroxide for Propulsion and Power," 35th AIAA/ASME/SAE/ASEE Joint Propulsion Conference and Exhibit, Aliso Viejo, CA, AIAA Paper 1999-2880, June 1999.

[4] Ventura, M., Wernimont, E., Heister, S., and Yuan, S., "Rocket Grade Hydrogen Peroxide (RGHP) for Use in Propulsion and Power Devices-Historical Discussion of Hazards," 43rd AIAA/ASME/SAE/ASEE Joint Propulsion Conference and Exhibit, Cincinnati, OH, AIAA Paper 2007-5468, July 2007.

[5] Unger, R. J., "NASA Hydrogen Peroxide Propulsion Perspective," *5th International Hydrogen Peroxide Propulsion Conference*, Purdue Univ., West Lafayette, IN, Sept. 2002, pp. 245–255.

[6] Wernimont, E. J., "Hydrogen Peroxide Catalyst Beds: Lighter and Better Than Liquid Injectors," 41st AIAA/ASME/SAE/ASEE Joint Propulsion Conference and Exhibit, Tucson, AZ, AIAA Paper 2005-4455, July 2005.

[7] Coxhill, I., Richardson, G., and Sweeting, M., "An Investigation of a Low Cost HTP/Kerosene 40 N Thruster for Small Satellite," 38th AIAA/ASME/SAE/ASEE Joint Propulsion Conference and Exhibit, Indianapolis, IN, AIAA Paper 2002-4155, July 2002.

[8] Sisco, J., Austin, B. L., Mok, J. S., and Anderson, W. E., "Autoignition of Kerosene by Decomposed Hydrogen Peroxide in a Dump-Combustor Configuration," *Journal of Propulsion and Power*, Vol. 21, No. 3, 2005, pp. 450–459.
doi:10.2514/1.5287

[9] Sadov, V. N., "Ignition of Kerosene and Hydrogen Peroxide in Combustion Chamber by Fire Jet," *3rd International Conference on Green Propellant for Space Propulsion* [CD-ROM], Poitiers, France, SP-635, ESA Publication Div., Noordwijk, The Netherlands, Sep. 2006.

[10] Cong, Y., Zhang, T., Li, T., Sun, J., Wang, X., Ma, L., Liang, D., and Lin, L., "Propulsive Performance of a Hypergolic H_2O_2/Kerosene Bipropellant," *Journal of Propulsion and Power*, Vol. 20, No. 1, 2004, pp. 83–86.
doi:10.2514/1.9189

[11] Pourpoint, T. L., "Hypergolic Ignition of a Catalytically Promoted Fuel with Rocket Grade Hydrogen Peroxide," Ph.D. Thesis, School of Aeronautics and Astronautics, Purdue Univ., West Lafayette, IN, 2005.

[12] Austin, B. L., Heister, S. D., and Anderson, W. E., "Characterization of Pintle Engine Performance for Nontoxic Hypergolic Bipropellants," *Journal of Propulsion and Power*, Vol. 21, No. 4, 2005, pp. 627–635.
doi:10.2514/1.7988

[13] Andrews, D., and Sunley, H., "The Gamma Rocket Engines for Black Knight," *Journal of the British Interplanetary Society*, Vol. 43, Jul. 1990, pp. 301–310.

[14] Ventura, M. C., and Wernimont, E. J., "History of the Reaction Motors Super Performance 90 percent H_2O_2/Kerosene LR-40 Rocket Engine," 37th AIAA Joint Propulsion Conference and Exhibit, Salt Lake, UT, AIAA Paper 2001-3838, July 2001.

[15] Walder, H., and Purchase, L. J., "The Influence of Injector Design on the Thermal Ignition of Hydrogen Peroxide and Kerosene," Royal Aircraft Establishment, RAE-TN-RPD-80, Hampshire, England, U.K., Apr. 1953.

[16] Kappenstein, C., Pirault-Roy, L., Guerin, M., Wahdan, T., Ali, A. A., Al-Sagheer, F. A., and Zaki, M. I., "Monopropellant Decomposition Catalysts. V. Thermal Decomposition and Reduction of Permanganates as Models for the Preparation of Supported MnOx Catalysts," *Applied Catalysis A: General*, Vol. 234, Nos. 1–2, 2002, pp. 145–153.
doi:10.1016/S0926-860X(02)00220-X

[17] Tian, H., Zhang, T., Sun, X., Liang, D., and Lin, L., "A Novel Mixed Metal Oxide Catalyst for the Decomposition of Hydrogen Peroxide," *2nd International Hydrogen Peroxide Propulsion Conference*, West Lafayette, IN, ESA Publication Div., Noordwijk, The Netherlands, 1999, pp. 199–208.

[18] An, S., Brahmi, R., Kappenstein, C., and Kwon, S., "Transient Behavior of H_2O_2 Thruster: Effect of Injector Type and Ullage Volume," *Journal of Propulsion and Power*, Vol. 25, No. 6, 2009, pp. 1357–1360.
doi:10.2514/1.46731

[19] An, S., and Kwon, S., "Scaling and Evaluation of Pt/Al2O3 Catalytic

Reactor for Hydrogen Peroxide Monopropellant Thruster," *Journal of Propulsion and Power*, Vol. 25, No. 5, 2009, pp. 1041–1045.
doi:10.2514/1.40822

[20] Gordon, S., and McBride, B. J., "Computer Program for Calculation of Complex Chemical Equilibrium Compositions and Applications," NASA Ref. Publ. 1311, 1994.

[21] "Propellant, Hydrogen Peroxide," U.S. Department of Defense, Performance Specification MIL-PRF-16005F, 2003.

[22] Coleman, H. W., and Steele, W. G., *Experimentation and Uncertainty Analysis for Engineers*, 2nd ed., Wiley, New York, 1999, pp. 47–82.

E. Kim
Associate Editor